OPEN

Correspondence and
requests for materials
should be addressed to
G.Q.X. (xiegq@sjtu.
edu.cn)

Wavelength-Versatile Graphene-Gold Film Saturable Absorber Mirror for Ultra-Broadband Mode-Locking of Bulk Lasers

Jie Ma[1], Guoqiang Xie[1], Peng Lv[2], Wenlan Gao[1], Peng Yuan[1], Liejia Qian[1], Uwe Griebner[3], Valentin Petrov[3], Haohai Yu[4], Huaijin Zhang[4] & Jiyang Wang[4]

[1]Key Laboratory for Laser Plasmas (Ministry of Education), Department of Physics and Astronomy, Shanghai Jiao Tong University, Shanghai 200240, China, [2]School of Electronic Science and Applied Physics, Hefei University of Technology, Hefei 230009, China, [3]Max Born Institute for Nonlinear Optics and Ultrafast Spectroscopy, Max-Born-Str. 2a, D-12489 Berlin, Germany, [4]State Key Laboratory of Crystal Materials, Shandong University, Jinan 250100, China.

An ultra-broadband graphene-gold film saturable absorber mirror (GG-SAM) with a spectral coverage exceeding 1300 nm is experimentally demonstrated for mode-locking of bulk solid-state lasers. Owing to the p-type doping effect caused by graphene-gold film interaction, the graphene on gold-film substrate shows a remarkably lower light absorption relative to pristine graphene, which is very helpful to achieve continuous-wave mode-locking in low-gain bulk lasers. Using the GG-SAM sample, stable mode-locking is realized in a Yb:YCOB bulk laser near 1 μm, a Tm:CLNGG bulk laser near 2 μm and a Cr:ZnSe bulk laser near 2.4 μm. The saturable absorption is characterised at an intermediate wavelength of 1.56 μm by pump-probe measurements. The as-fabricated GG-SAM with ultra-broad bandwidth, ultrafast recovery time, low absorption, and low cost has great potential as a universal saturable absorber mirror for mode-locking of various bulk lasers with unprecedented spectral coverage.

Ultrashort pulse lasers have become important tools in scientific research, medical imaging, high-capacity communication, and industrial processing[1]. Passive mode-locking is the general and direct approach employed to generate ultrashort pulses. In passively mode-locked lasers, a saturable absorber is usually required to initiate and sustain mode-locking operation. Thus far, semiconductor saturable absorber mirrors (SESAMs) based on quantum wells have been widely used as passive mode-lockers in the near-infrared spectral region; however, SESAMs generally have a limited operational bandwidth and require a complicated fabrication process. Furthermore, SESAMs fabrication technique near and above 2 μm is a big challenge, which limits the development and applications of mid-infrared mode-locked lasers. In recent years, single-walled carbon nanotubes (SWCNTs) become a potential alternative as ultrafast saturable absorbers[2–7]. The absorption bands of SWCNTs depend on their diameter and chirality; however, nanotubes with well-defined diameters and chirality are difficult to synthesise. Moreover, the available diameters and chirality of current SWCNTs cannot support operation beyond 2.1 μm[7,8]. In addition, significant scattering losses due to the bundling and curling of nanotubes limit their applications[4].

Graphene, a single-atom-thin sheet of carbon with a honeycomb lattice, has attracted great interest since its discovery in 2004 because of its unique electronic, photonic, mechanical, and thermal characteristics as well as its extensive and exciting application prospects[9–12]. Previous studies have indicated that pristine graphene has a universal linear optical absorption of 2.293% per layer in the visible-to-infrared spectral range and this absorption is independent of optical frequency[13–15]. Saturable absorption in graphene has been observed as a result of Pauli blocking of electron states[16]. Moreover, graphene has the additional advantages of ultrafast recovery time[17–20], low saturation energy fluence, large Kerr nonlinearity effect[21], low cost, and easy fabrication. Compared to SESAMs and SWCNTs mentioned above, graphene has a zero band-gap and exhibits linear dispersion near Dirac point[22]; thus, graphene saturable absorbers can theoretically operate over an ultrabroad spectral range covering in practice all known ultrashort pulse lasers[11,16,23–25]. However, graphene cannot be self-supported and it must be transferred onto optical substrate when used as saturable absorber, thus the real operation bandwidth of graphene saturable

absorber is usually limited by the bandwidth of the substrate. For example, at present the dielectric reflective films generally have a bandwidth of 100–300 nm, thus the graphene-dielectric-film-based saturable absorber can only have similar operation bandwidth[26–28]. So far, graphene mode-locking of fiber and bulk lasers has been reported by transferring graphene onto fiber end surface[16], dielectric film mirrors[26–28], and uncoated quartz mirrors[29–31], in these cases graphene shows an intrinsic optical absorption of ~2.3% per layer. A round trip intracavity loss of 4.6% or even larger is not a problem for high-gain fiber lasers, but it is desirable to tailor and reduce the absorption loss for low-gain bulk lasers.

In this paper, we experimentally demonstrate a low-absorption, ultra-broadband graphene-gold film saturable absorber mirror (GG-SAM) with a spectral coverage exceeding 1300 nm. In the GG-SAM, the optical absorption of graphene is significantly reduced by p-type doping effect of gold film, and the ultra-broad operation bandwidth of GG-SAM is achieved benefitting from the ultra-broadband reflection of gold film. Using the same GG-SAM sample, we have achieved stable mode-locking of bulk lasers at wavelengths near 1, 2, and 2.4 μm, and experimentally demonstrated saturable absorption of the GG-SAM at 1.56 μm by pump-probe measurements. The as-fabricated GG-SAM shows good potential as a wavelength-versatile saturable absorber for ultrafast bulk lasers at various wavelengths.

Results

Characteristics of GG-SAM. The structure of the GG-SAM is schematically shown in Figure 1a. The GG-SAM consists of a BK7 glass substrate, a gold film layer, and few layers of graphene. The 120-nm-thick gold film layer ensures high reflectivity from the near- to the far-infrared band. Graphene is grown on Cu foil by chemical vapour deposition (CVD) and then transferred onto the gold-film substrate. The graphene layer has a large area of ~1 cm², which facilitates optical characterisation and laser applications. Figure 1b shows a photograph of the fabricated GG-SAM, where the graphene layer can be identified by the naked eye.

The reflectivity spectra of the GG-SAM and gold-film substrate are shown in Figure 2. For comparison, the transmission spectrum of monolayer graphene on quartz substrate is also displayed in the same figure. Ultra-broadband absorption of the GG-SAM can be observed from ~800 nm to ~2200 nm. We observe only little deviation from the universal absorption of ~2.3% for graphene on quartz substrate
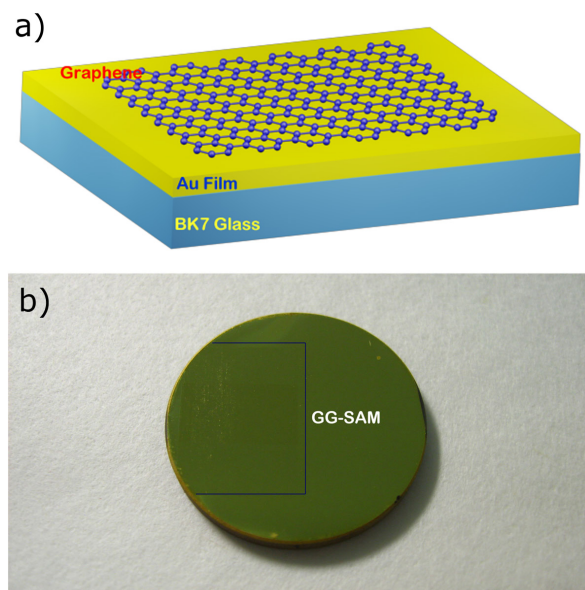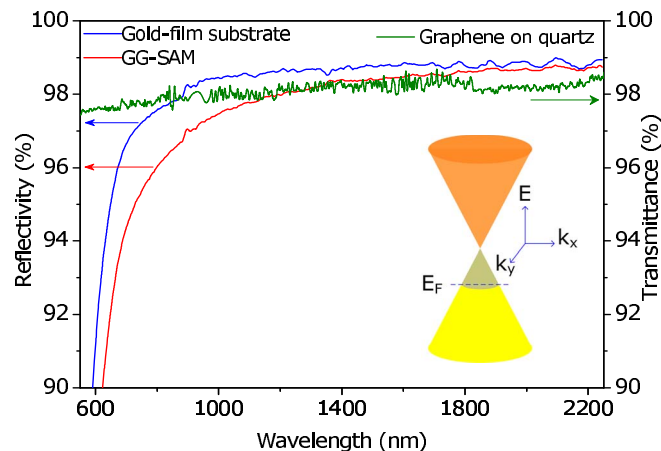

Figure 2 | **The reflectivity spectra of GG-SAM and gold-film substrate, and transmission spectrum of monolayer graphene on quartz substrate.** Inset: the energy band diagram of the p-type doped graphene. The p-type doping effect results in a downward shift of Fermi level.

at low photon energy, which may be caused by many-body effects[32,33]. Compared to graphene on quartz substrate, the GG-SAM shows much lower optical absorption from near-infrared to mid-infrared, which indicates graphene–gold film interaction[32,34,35]. When graphene contacts with gold film, it is p-type doped by the gold film, which causes the Fermi level to shift downward from the Dirac point, thereby forming a band-gap in graphene[36,37], as shown in the inset of Figure 2. The electrons in graphene behave as Dirac fermions[38] and follow the Fermi-Dirac distribution. Thus, at room temperature, the quantum states close to Fermi level are partly occupied by electrons. The electron population in the valence band far beyond the Fermi level for p-type doped graphene will be much lower than that in pristine graphene, which leads to the decreased absorption for the GG-SAM. It is worth noting that in the GG-SAM a polycrystalline gold film was used, and the p-type doping level is sensitive to the local surface structures of gold film and adsorption distance[39], thus the amount of Fermi level shift will be different at different doping domains and shows a distribution across the GG-SAM. Some absorption still exists at 2 μm and beyond. While low non-saturable part of the absorption improves the overall laser performance, low saturable absorption part is advantageous for mode-locking of low-gain bulk lasers, helping to suppress the Q-switching instability[40].

Raman spectroscopy offers a fast, unambiguous, and effective means to characterize the structure of graphene[41]. It has been demonstrated that the number of graphene layer can be estimated by Raman spectrum[41,42]. The recorded Raman spectrum of the GG-SAM excited by a 514-nm laser source is shown in Figure 3a. The Raman signal of graphene, which we obtained by subtracting the contribution of the gold-film substrate, is shown in Figure 3b. The two characteristic Raman peaks designated as G and 2D can be clearly observed. The G peak is located at ~1582 cm^{-1} with a full-width at half-maximum (FWHM) of approximately 24 cm^{-1}, and the 2D peak is at ~2689 cm^{-1} with a FWHM of approximately 55 cm^{-1}. The G and 2D peaks in Figure 3 are blue-shifted apparently relative to those in pristine graphene, in which G peak is at ~1580 cm^{-1} and 2D peak is at ~2680 cm^{-1} [43]. The observed blue-shift suggests p-type doping effect in graphene[43,44]. According to the Raman spectrum, the thickness of graphene on the GG-SAM is identified to be 2 layers[41,42]. In addition, the D peak at ~1349 cm^{-1} is very weak in Figure 3, which indicates low level of defects for the graphene on the gold-film substrate.

In order to investigate the ultrafast nonlinear optical characteristics of the GG-SAM, we performed pump-probe measurement. The laser source used for the pump-probe measurement was an Er-fiber
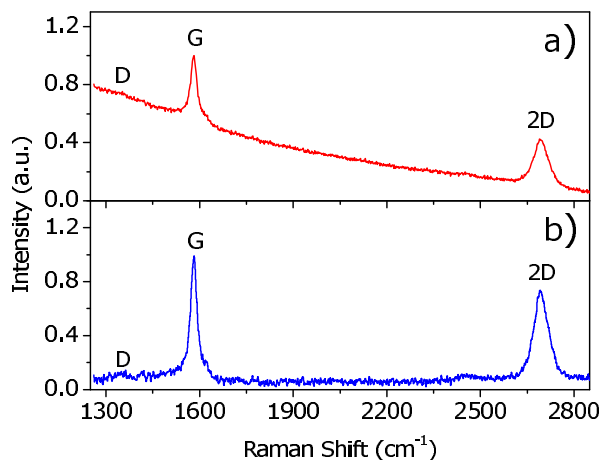

Figure 1 | (a) Design of the GG-SAM. (b) Photograph of the fabricated GG-SAM.

Figure 3 | (a) Raman spectrum of the GG-SAM. (b) Raman spectrum of graphene after subtraction of the contribution of the gold film substrate.

femtosecond laser operating at 1.56 μm. The recorded pump-probe trace shown in Figure 4, is fitted with a double-exponential kernel function. Saturable absorption in the GG-SAM can be clearly observed, with an ultrafast recovery time of ~180 fs related to electron-electron scattering and a slower component of ~1285 fs related to electron-hole recombination, electron-phonon interaction, and phonon bottleneck effect[20]. Pump-probe measurement result indicates that the GG-SAM has similar recovery time as pristine graphene at the same wavelength[31], suggesting that the ultrafast carrier kinetics of graphene is not sensitive to doping effect.

GG-SAM mode-locked bulk lasers. To assess the mode-locking performance of the ultra-broadband GG-SAM, we performed mode-locking experiments at wavelengths of 1, 2, and 2.4 μm. The mode-locking results obtained for a Yb:YCOB bulk laser near 1 μm are shown in Figure 5. With the GG-SAM as an end mirror, self-starting steady-state mode-locking was achieved. The recorded autocorrelation trace indicates mode-locked pulse duration of 152 fs. The spectrum is centered at 1037 nm, with a FWHM bandwidth of 10.2 nm. The time–bandwidth product of the mode-locked pulses was calculated to be approximately 0.43. The time–bandwidth product is a bit large for sech²-shaped pulses but it was impossible to maintain the stable stationary regime by further reduction of the intracavity group-velocity dispersion aiming at shorter pulses. The radio-frequency (RF) spectra in Figure 5c–d
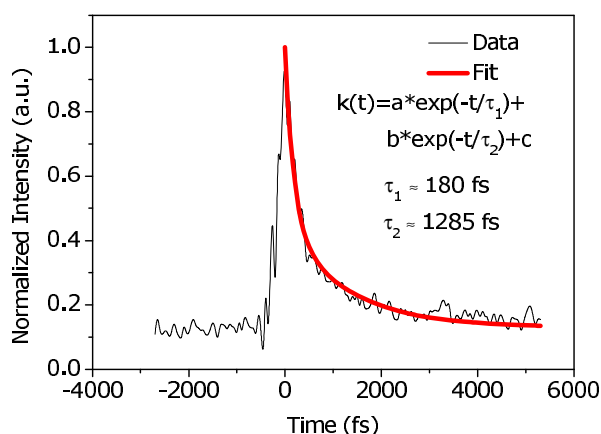

Figure 4 | Pump-probe measurement of the GG-SAM. The curve is fitted with a double-exponential kernel function with a fast (180 fs) and slow (1285 fs) time decay component.

show a high signal-to-noise ratio (~72 dBm) during mode-locking operation. In the experiment, we monitored the laser over two hours and it remained very stable, showing excellent mode-locking performance of the GG-SAM in the 1 μm spectral region.

Mode-locking experiments performed in a Tm:CLNGG bulk laser with the same GG-SAM sample indicated that self-starting steady-state mode-locking could also be achieved at 2010 nm. Figure 6a and 6b show the autocorrelation trace and the corresponding optical spectrum of the mode-locked pulses in this case. With a pulse duration (FWHM) of 354 fs and a spectral FWHM of 12.6 nm, the time-bandwidth product is 0.33, which is very close to the Fourier limit. The obtained pulses are significantly shorter compared to SESAM and pristine graphene mode-locking under similar conditions[27,45], indicating excellent mode locking performance of the GG-SAM. The radio-frequency spectrum in Figure 6c shows a high signal-to-noise ratio of 68 dBm, without any sign of Q-switching instability. Also in this case mode-locking could be sustained over two hours without deterioration of the laser performance.

To test the mode-locking capability of the GG-SAM at longer mid-infrared wavelength, we further performed a mode-locking experiment with the GG-SAM in a Cr:ZnSe bulk laser near 2.4 μm. Stable mode-locked pulses as short as 116 fs were obtained, as shown in Figure 7a. The mode-locked spectrum is centered at 2352 nm with a FWHM bandwidth of 50.2 nm (Figure 7b), corresponding to a time-bandwidth product of ~0.316. Figure 7c shows the radio-frequency spectrum of the mode locked laser indicating high stability. Limited by a slower response time (>3 ns) of the detector used, the RF spectrum shows a signal-to-noise ratio of about 50 dBm. We also conducted a wavelength tuning experiment in the mode-locked Cr:ZnSe laser. Benefitting from the broad bandwidth of the GG-SAM, a wide mode-locking tuning range of 116 nm from 2310 to 2426 nm was achieved, as shown in Figure 7d.

It is worth noting that graphene has a large Kerr nonlinear refractive index[21], the gain modulation induced by Kerr lens effect may cause mode-locking of lasers. In the experiment, when the laser beam was removed out of the graphene region, no mode-locking signal was observed. Thus it is convinced that the mode-locking is caused by the GG-SAM. In order to check Kerr lens effect of the GG-SAM, we numerically simulated the saturation gain modulation induced by Kerr lens effect of the GG-SAM[46,47]. The simulation results show that the gain modulation is about 0.1–0.2% for the three mode-locked lasers. Undoubtedly, Kerr-lens effect of the GG-SAM plays an important role in mode-locking of the lasers. Taking into account the saturable absorption of graphene, we believe that mode locking is the result of joint contribution of saturable absorption and Kerr lens effect of the GG-SAM. In the experiment, we also tried mode-locking by use of GG-SAM with monolayer, bilayer, and three-layer graphene. With monolayer graphene, it is difficult to initiate the mode locking. However, with bilayer or three-layer graphene, mode locking can be easily initiated, which implies that the modulation depth is larger with multiple-layer graphene.

Discussion

A low-absorption, ultra-broadband graphene-gold film saturable absorber mirror (GG-SAM) for mode-locking of bulk solid-state lasers has been experimentally demonstrated. In contrast to state-of-the-art commercial SESAMs, which have a limited operational bandwidth of ~100 nm, the GG-SAM has been successfully employed over a spectral range exceeding 1300 nm, as evidenced by stable mode-locking of a Yb:YCOB laser near 1 μm, a Tm:CLNGG laser near 2 μm and a Cr:ZnSe laser near 2.4 μm. Due to the ultra-broadband saturable absorption of graphene and ultra-broadband reflectivity of gold film, it is possible for the GG-SAM to operate at longer mid-infrared wavelength, at which SESAMs and SWCNTs are not available. In none of the lasers studied did we observe any signs of self mode-locking under identical con-
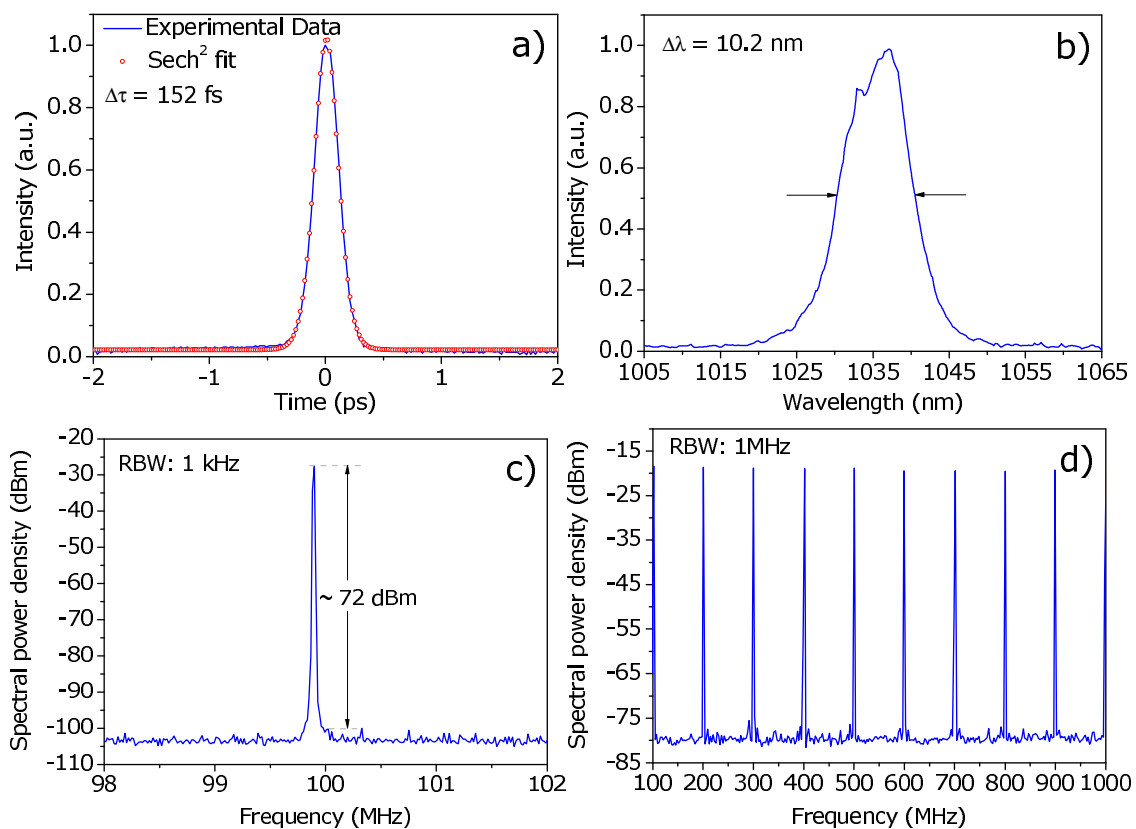
Figure 5 | **Mode-locking results obtained with the GG-SAM at the wavelength of 1 μm.** (a) Autocorrelation trace. (b) Optical spectrum. (c) Radio-frequency spectrum with 1 kHz resolution. (d) Radio-frequency spectrum with 1 GHz span.
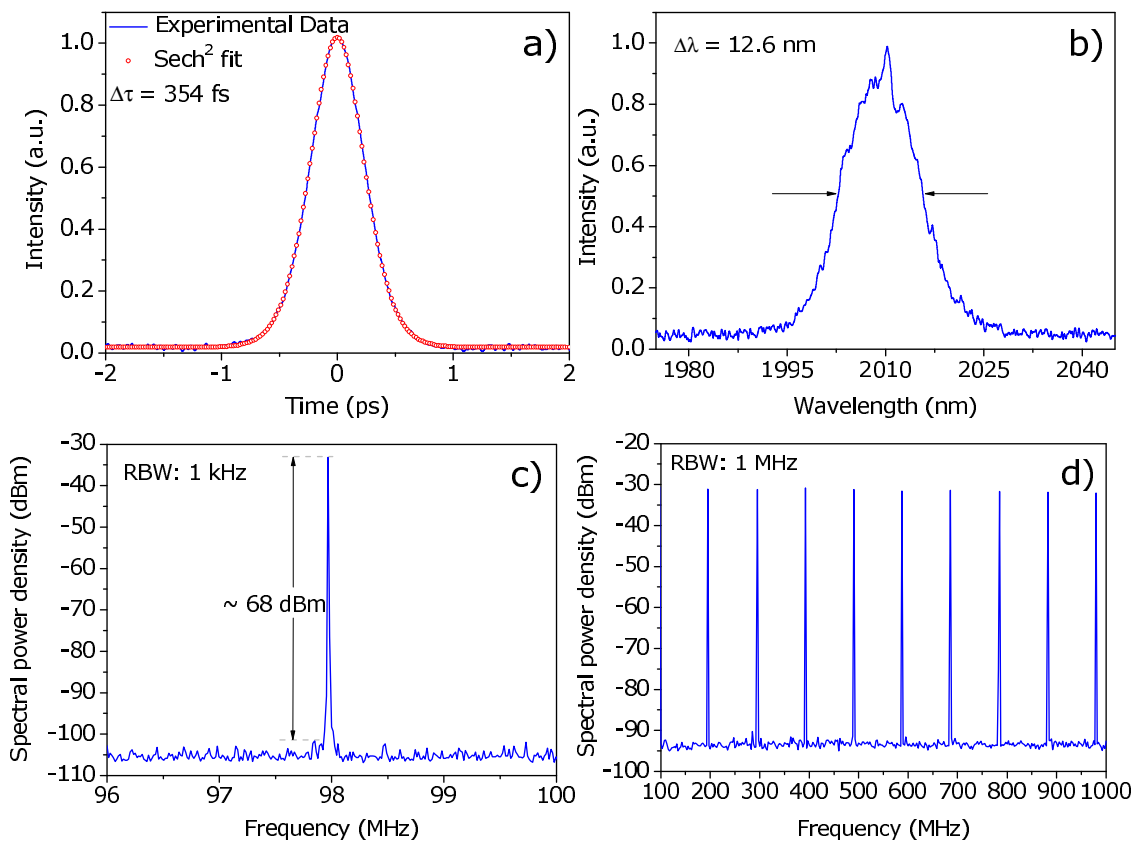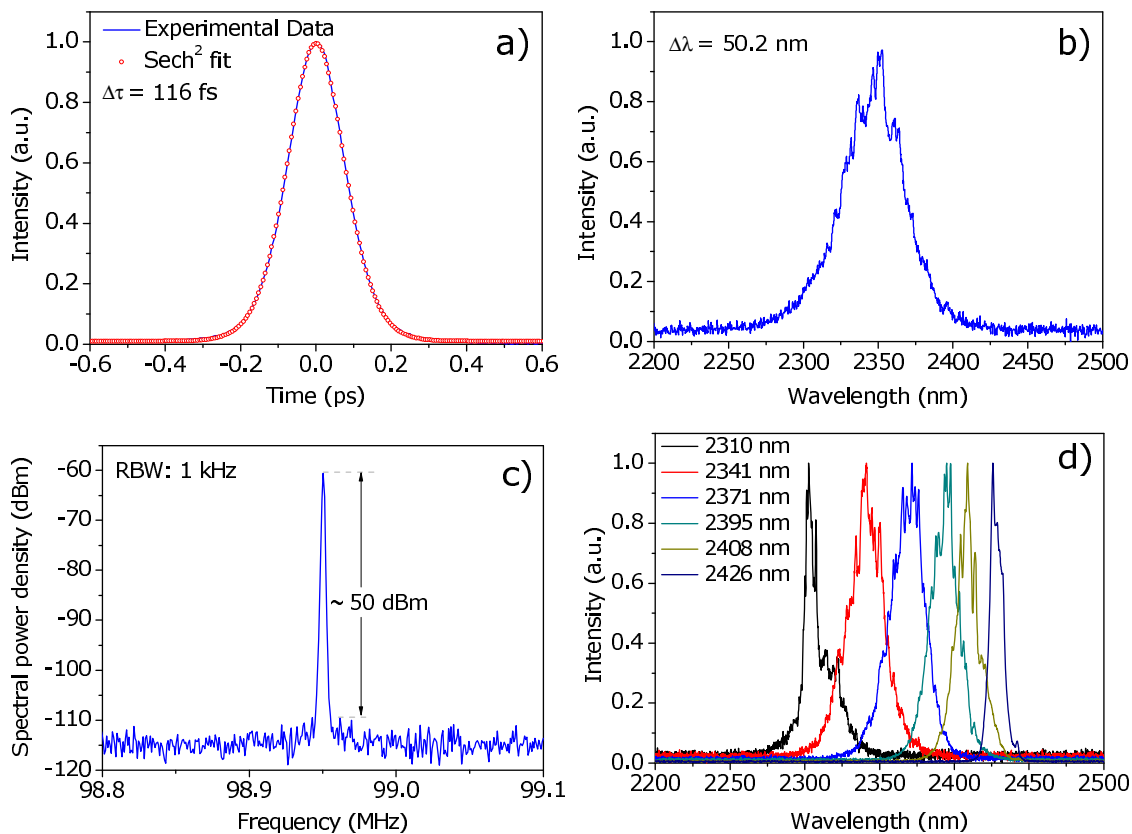

Figure 6 | **Mode-locking results obtained with the GG-SAM at 2 μm wavelength.** (a) Autocorrelation trace. (b) Optical spectrum. (c) Radio-frequency spectrum with 1 kHz resolution. (d) Radio-frequency spectrum with 1 GHz span.

Figure 7 | Mode-locking results obtained with the GG-SAM near 2.4 μm. (a) Autocorrelation trace. (b) Optical spectrum. (c) Radio-frequency spectrum with 1 kHz resolution. (d) Tunable mode-locking spectra of the Cr:ZnSe laser.

ditions without the GG-SAM. We also show that the optical absorption of graphene in GG-SAM is significantly reduced due to p-type doping effect, which makes the GG-SAM more suitable for mode-locking of low-gain bulk lasers. The developed GG-SAM with ultra-broad bandwidth, ultrafast recovery time, low absorption, and low cost has great potential as a universal saturable absorber for ultrafast bulk lasers at various wavelengths.

Methods

GG-SAM fabrication. Graphene flakes were synthesised on Cu foil at 1000°C via the CVD method using a gas mixture of methane and hydrogen. Subsequently, 5 at.% polymethylmethacrylate (PMMA) in chlorobenzene was spin-coated onto the graphene. The graphene-Cu substrate was then immersed in Marble's reagent solution for several hours until the Cu substrate was completely etched. After that, the PMMA-supported graphene film was washed in deionised water and transferred onto the gold-film substrate. After drying, the PMMA film on the graphene-gold film substrate was dissolved and removed with acetone solution. The fabricated graphene-gold film substrate was characterised and used as saturable absorber mirror in laser experiments.

Mode-locking experiments. A schematic of the mode-locked laser at the wavelength of 1 μm is shown in Figure 8. A standard X-folded cavity was employed, and the GG-SAM was installed as an end mirror of the cavity. The gain medium was a Yb:YCOB crystal pumped by a 980-nm single-emitter laser diode. A pair of SF10 prisms was used for dispersion compensation. The transmission of the output coupler at the laser wavelength was 2%. The cavity length was ~1.50 m, corresponding to a pulse repetition rate of ~99.9 MHz. The average output power of the Yb:YCOB mode-locked laser was ~53 mW under an incident pump power of ~1.3 W. The relatively low optical-to-optical efficiency of ~4% was attributed to poor mode-matching between pump spot and laser mode.

The laser setups employed for mode-locking of Tm:CLNGG and Cr:ZnSe bulk lasers were very similar to that used for the Yb:YCOB laser. A pair of CaF$_2$ prisms was used to compensate for dispersion in the Tm:CLNGG and Cr:ZnSe lasers. For the mode-locked Tm:CLNGG laser, the transmission of the output coupler was 2%. Pumped by a 790-nm single-emitter laser diode, this laser emitted a maximum average output power of 97 mW under an incident pump power of ~2.1 W, and the average output power was much higher compared to the pristine graphene mode-locked laser under similar conditions[27]. For the Cr:ZnSe laser, the employed output coupler had a transmission of 3%. Pumping with a home-made Er,Yb:fiber laser at 1.56 μm, the mode-locked Cr:ZnSe laser generated an average output power of ~66 mW under an incident pump power of ~4.6 W. The low laser efficiency was mainly due to poor optical quality of the available Cr:ZnSe crystal. The wavelength tuning experiment was conducted by inserting a slit near the output coupler. By adjusting the slit, the wavelength tuning could be realized in mode locking operation. Output power of the above mode-locked lasers was limited only in one case by damage of the GG-SAM – in the Tm:CLNGG laser we observed such damage at a pulse fluence of ~1.9 mJ/cm^2.
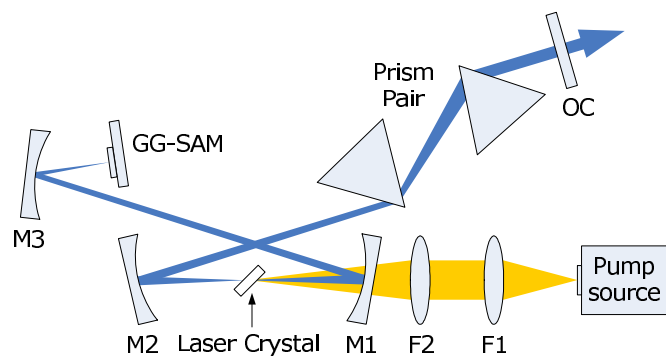

Figure 8 | Schematic of the mode-locked lasers. Mirrors M1, M2, and M3 have the same radius of curvature (ROC) of −100 mm. OC: output coupler. GG-SAM: graphene-gold film saturable absorber mirror.

1. Keller, U. Recent developments in compact ultrafast lasers. *Nature* **424**, 831–838 (2003).
2. Schibli, T. *et al.* Ultrashort pulse-generation by saturable absorber mirrors based on polymer-embedded carbon nanotubes. *Opt. Express* **13**, 8025–8031 (2005).
3. Hasan, T. *et al.* Nanotube–Polymer Composites for Ultrafast Photonics. *Adv. Mater.* **21**, 3874–3899 (2009).
4. Wang, F. *et al.* Wideband-tuneable, nanotube mode-locked, fibre laser. *Nat Nano* **3**, 738–742 (2008).

5. Cho, W. B. et al. Boosting the Non Linear Optical Response of Carbon Nanotube Saturable Absorbers for Broadband Mode-Locking of Bulk Lasers. Adv. Funct. Mater. **20**, 1937–1943 (2010).

6. Ferrari, S. et al. Optimizing Single-Walled-Carbon-Nanotube-Based Saturable Absorbers for Ultrafast Lasers. Adv. Funct. Mater. **22**, 4369–4375 (2012).

7. Schmidt, A. et al. 175 fs Tm:Lu$_2$O$_3$ laser at 2.07 μm mode-locked using single-walled carbon nanotubes. Opt. Express **20**, 5313–5318 (2012).

8. Cizmeciyan, M. N. et al. Graphene mode-locked femtosecond Cr:ZnSe laser at 2500 nm. Opt. Lett. **38**, 341–343 (2013).

9. Novoselov, K. S. et al. Electric Field Effect in Atomically Thin Carbon Films. Science **306**, 666–669 (2004).

10. Bonaccorso, F., Sun, Z., Hasan, T. & Ferrari, A. C. Graphene photonics and optoelectronics. Nat Photon **4**, 611–622 (2010).

11. Novoselov, K. S. et al. A roadmap for graphene. Nature **490**, 192–200 (2012).

12. Bao, Q. & Loh, K. P. Graphene Photonics, Plasmonics, and Broadband Optoelectronic Devices. ACS Nano **6**, 3677–3694 (2012).

13. Nair, R. R. et al. Fine Structure Constant Defines Visual Transparency of Graphene. Science **320**, 1308 (2008).

14. Stauber, T., Peres, N. M. R. & Geim, A. K. Optical conductivity of graphene in the visible region of the spectrum. Phys. Rev. B **78**, 085432 (2008).

15. Dawlaty, J. M. et al. Measurement of the optical absorption spectra of epitaxial graphene from terahertz to visible. Appl. Phys. Lett. **93**, 131905–131903 (2008).

16. Bao, Q. et al. Atomic-Layer Graphene as a Saturable Absorber for Ultrafast Pulsed Lasers. Adv. Funct. Mater. **19**, 3077–3083 (2009).

17. Sun, D. et al. Ultrafast Relaxation of Excited Dirac Fermions in Epitaxial Graphene Using Optical Differential Transmission Spectroscopy. Phys. Rev. Lett. **101**, 157402 (2008).

18. Xing, G., Guo, H., Zhang, X., Sum, T. C. & Huan, C. H. A. The Physics of ultrafast saturable absorption in graphene. Opt. Express **18**, 4564–4573 (2010).

19. Dawlaty, J. M., Shivaraman, S., Chandrashekhar, M., Rana, F. & Spencer, M. G. Measurement of ultrafast carrier dynamics in epitaxial graphene. Appl. Phys. Lett. **92**, 042116–042113 (2008).

20. Breusing, M. et al. Ultrafast nonequilibrium carrier dynamics in a single graphene layer. Phys. Rev. B **83**, 153410 (2011).

21. Zhang, H. et al. Z-scan measurement of the nonlinear refractive index of graphene. Opt. Lett. **37**, 1856–1858 (2012).

22. Ando, T. The electronic properties of graphene and carbon nanotubes. NPG Asia Mater **1**, 17–21 (2009).

23. Sun, Z. et al. Graphene Mode-Locked Ultrafast Laser. ACS Nano **4**, 803–810 (2010).

24. Bao, Q. et al. Graphene–Polymer Nanofiber Membrane for Ultrafast Photonics. Adv. Funct. Mater. **20**, 782–791 (2010).

25. Bao, Q. et al. Monolayer graphene as a saturable absorber in a mode-locked laser. Nano Res. **4**, 297–307 (2011).

26. Xu, J.-L. et al. Graphene saturable absorber mirror for ultra-fast-pulse solid-state laser. Opt. Lett. **36**, 1948–1950 (2011).

27. Ma, J. et al. Graphene mode-locked femtosecond laser at 2 μm wavelength. Opt. Lett. **37**, 2085–2087 (2012).

28. Xie, G. Q. et al. Graphene saturable absorber for Q-switching and mode locking at 2 μm wavelength [Invited]. Opt. Mater. Express **2**, 878–883 (2012).

29. Tan, W. D. et al. Mode locking of ceramic Nd:yttrium aluminum garnet with graphene as a saturable absorber. Appl. Phys. Lett. **96**, 031106–031103 (2010).

30. Cho, W. B. et al. High-quality, large-area monolayer graphene for efficient bulk laser mode-locking near 1.25 μm. Opt. Lett. **36**, 4089–4091 (2011).

31. Di Dio Cafiso, S. D. et al. Sub-100-fs Cr:YAG laser mode-locked by monolayer graphene saturable absorber. Opt. Lett. **38**, 1745–1747 (2013).

32. Mak, K. F. et al. Measurement of the Optical Conductivity of Graphene. Phys. Rev. Lett. **101**, 196405 (2008).

33. Mishchenko, E. G. Effect of Electron-Electron Interactions on the Conductivity of Clean Graphene. Phys. Rev. Lett. **98**, 216801 (2007).

34. Giovannetti, G. et al. Doping Graphene with Metal Contacts. Phys. Rev. Lett. **101**, 026803 (2008).

35. Wang, Q. H. et al. Understanding and controlling the substrate effect on graphene electron-transfer chemistry via reactivity imprint lithography. Nat Chem **4**, 724–732 (2012).

36. Malec, C. E. & Davidović, D. Electronic properties of Au-graphene contacts. Phys. Rev. B **84**, 033407 (2011).

37. Sławińska, J., Dabrowski, P. & Zasada, I. Doping of graphene by a Au(111) substrate: Calculation strategy within the local density approximation and a semiempirical van der Waals approach. Phys. Rev. B **83**, 245429 (2011).

38. Novoselov, K. S. et al. Two-dimensional gas of massless Dirac fermions in graphene. Nature **438**, 197–200 (2005).

39. Sławińska, J., Wlasny, I., Dabrowski, P., Klusek, Z. & Zasada, I. Doping domains in graphene on gold substrates: First-principles and scanning tunneling spectroscopy studies. Phys. Rev. B **85**, 235430 (2012).

40. Hönninger, C., Paschotta, R., Morier-Genoud, F., Moser, M. & Keller, U. Q-switching stability limits of continuous-wave passive mode locking. J. Opt. Soc. Am. B **16**, 46–56 (1999).

41. Ferrari, A. C. et al. Raman Spectrum of Graphene and Graphene Layers. Phys. Rev. Lett. **97**, 187401 (2006).

42. Graf, D. et al. Spatially Resolved Raman Spectroscopy of Single- and Few-Layer Graphene. Nano Lett. **7**, 238–242 (2007).

43. Wang, W. X. et al. The study of interaction between graphene and metals by Raman spectroscopy. J. Appl. Phys. **109**, 07C501–503 (2011).

44. Das, A. et al. Monitoring dopants by Raman scattering in an electrochemically top-gated graphene transistor. Nat Nano **3**, 210–215 (2008).

45. Ma, J. et al. Diode-pumped mode-locked femtosecond Tm:CLNGG disordered crystal laser. Opt. Lett. **37**, 1376–1378 (2012).

46. Liu, K. X. et al. Kerr lens mode locking of a diode-pumped Nd:YAG laser. Opt. Lett. **17**, 1361–1363 (1992).

47. Xie, G. Q. et al. High-power self-mode-locked Yb:Y2O3 ceramic laser. Opt. Lett. **32**, 2741–2743 (2007).

Acknowledgments

Author contributions

J.M., G.X. and L.Q. designed the experiment and wrote the paper. J.M., W.G. and P.Y. performed device fabrication and laser experiments. P.L. synthesised the graphene. U.G. and V.P. performed the pump-probe measurements of the GG-SAM. H.Y., H.Z. and J.W. fabricated the laser crystals. G.X. supervised the project. All authors discussed the results and commented on the manuscript.

Additional information

Competing financial interests: The authors declare no competing financial interests.

How to cite this article: Ma, J. et al. Wavelength-Versatile Graphene-Gold Film Saturable Absorber Mirror for Ultra-Broadband Mode-Locking of Bulk Lasers. Sci. Rep. **4**, 5016; DOI:10.1038/srep05016 (2014).